

Effect of Signal Peptide on the Stability and Folding Kinetics of Maltose Binding Protein[†]

K. Beena,[‡] Jayant B. Udgaonkar,[§] and R. Varadarajan^{*,‡}

Molecular Biophysics Unit, Indian Institute of Science, Bangalore 560 012, India, and National Centre for Biological Sciences, Tata Institute of Fundamental Research, GKVK Campus, Bangalore 560 065, India

Received November 17, 2003; Revised Manuscript Received January 22, 2004

ABSTRACT: While the role of the signal sequence in targeting proteins to specific subcellular compartments is well characterized, there are fewer studies that characterize its effects on the stability and folding kinetics of the protein. We report a detailed characterization of the folding kinetics and thermodynamic stabilities of maltose binding protein (MBP) and its precursor form, preMBP. Isothermal GdmCl and urea denaturation as a function of temperature and thermal denaturation studies have been carried out to compare stabilities of the two proteins. preMBP was found to be destabilized by about 2–6 kcal/mol (20–40%) with respect to MBP. Rapid cleavage of the signal peptide by various proteases shows that the signal peptide is accessible in the native form of preMBP. The observed rate constant of the major slow phase in folding was decreased 5-fold in preMBP relative to MBP. The rate constants of unfolding were similar at 25 °C, but preMBP also exhibited a large burst phase change in unfolding that was absent in MBP. At 10 °C, preMBP exhibited a higher unfolding rate than MBP as well as a large burst phase. The appreciable destabilization of MBP by signal peptide is functionally relevant, because it enhances the likelihood of finding the protein in an unfolded translocation-competent form and may influence the interactions of the protein with the translocation machinery. Destabilization is likely to result from favorable interactions between the hydrophobic signal peptide and other hydrophobic regions that are exposed in the unfolded state.

A significant subset of proteins in both prokaryotes and eukaryotes needs to be exported to their site of action from the cytosol, the usual site of protein synthesis. Many of these exported proteins are synthesized in a precursor form (pre-proteins) with an additional, N-terminal amino acid extension called a signal peptide. Signal peptides consist of short stretches of nearly 15–40 amino acids. After delivery of the protein to the correct subcellular compartment, they are normally removed by specialized membrane-associated signal peptidases (1). The significance of the signal peptide in protein translocation and secretion as a target recognition motif is a well-established concept (1, 2), but its role in directly modulating the properties of the pre-proteins themselves and hence the export process is not as well characterized.

The earliest studies on signal peptides were related mainly to their direct interaction with the membrane for protein insertion into and across the membrane barrier (3–5). Park et al. first reported the involvement of the signal peptide in the folding of the precursor proteins of maltose binding

protein (MBP) and ribose binding protein (RBP) (6). Subsequently, there have been very few studies that report a quantitative comparison of thermodynamic and kinetic properties of a pre-protein and the corresponding mature protein (7, 8).

Previous comparisons of precursor and mature forms of MBP have mainly focused on the folding rates of the two proteins using the relaxation time measured in the manual mixing experiments (9–11), but an exhaustive, quantitative comparison of folding kinetics of the two proteins is not available. No direct measurement of the relative stability of the precursor form and the mature forms have been carried out. Stability studies have only been reported with mutants of the mature protein which are known to refold at rates similar to the precursor form or with slow folding suppressor mutants of export defective preMBP (12). In the current work, we report a complete thermodynamic and kinetic comparison between the precursor and the mature forms of an *Escherichia coli* protein MBP.

MBP is a large, two domain, 370-residue periplasmic protein involved in maltose uptake and chemotaxis. It is synthesized in the cytosol as a pre-protein containing a 26-residue signal peptide at the N-terminus (preMBP). Wild type preMBP is difficult to isolate in large amounts because it is

[†] This work was supported by grants from Department of Biotechnology (DBT) and Department of Science and Technology (DST) to R.V. R.V. and J.B.U. are recipients of Swarnajayanti Fellowship (Government of India) and of Senior Research Fellowships from the Wellcome Trust.

* Corresponding author. Molecular Biophysics Unit, Indian Institute of Science, Bangalore, 560 012 India. Phone: 011-91-80-2932612. Fax: 91-80-3600535 or 91-80-3600683. E-mail: varadar@mbu.iisc.ernet.in.

[‡] Indian Institute of Science.

[§] Tata Institute of Fundamental Research.

¹ Abbreviations: MBP, maltose binding protein; preMBP, precursor MBP with signal peptide; CGH10, citrate, glycine, and HEPES buffer (10 mM each); GdmCl, guanidinium chloride; CD, circular dichroism; T_m , temperature of maximal heat capacity; ANS, 8-anilino-1-naphthalenesulphonic acid; C_m , denaturant concentration at which unfolded protein population is 50%; wt, wild type.

readily cleaved by signal peptidase *in vivo* to generate the mature protein. Hence, we have used a mutant of preMBP carrying a mutation in the signal peptide, A14EpreMBP, as a substitute for authentic preMBP. This mutant has already been reported to be identical to the authentic preMBP with respect to its refolding and unfolding relaxation times (9) and interaction with SecB (13). In the present work, isothermal GdmCl, urea denaturation, and thermal denaturation studies have been carried out to compare the stabilities of the proteins. Folding/unfolding kinetics have been monitored using circular dichroism and fluorescence measurements. This study clearly reveals that the signal peptide affects the stability as well as the folding and unfolding kinetics of MBP to a greater extent than previously appreciated.

preMBP is a substrate for the *E. coli* chaperone SecB. The cytosolic chaperone SecB binds to pre-proteins and maintains them in a translocation-competent state (14). A number of studies have examined the interaction of SecB with physiological as well as model substrates (10, 15–17). However, a detailed quantitative understanding of the relative importance of kinetic and thermodynamic factors in SecB/substrate interactions is still to be achieved. From manual mixing experiments, preMBP is known to fold more slowly than MBP (6). Since SecB binding occurs in competition with the substrate folding, slower folding substrates are more likely to bind to SecB. While it is known that the signal peptide slows down the folding of MBP, the molecular basis of this effect has been unclear. The present studies suggest that the signal peptide stabilizes the unfolded state as well as the collapsed intermediate(s) and thereby decreases the refolding rate.

EXPERIMENTAL PROCEDURES

Materials. Maltose, PMSF, IPTG, ampicillin, trisodium citrate, glycine, papain, trypsin, chymotrypsin, subtilisin, proteinase K, fast flow Q-Sepharose, ANS, and SephadexG75 were from Sigma. HEPES and ultrapure GdmCl were purchased from USB. Amylose resin was obtained from NEB. All the other chemicals were from local commercial sources and were of analytical reagent quality.

Methods. Strains, Plasmids, and Protein Purification. The MBP-deficient strain POP6590 harboring the plasmid pMAL-P2-MBP (18) was used as a source of MBP and preMBP. The mutant A14EpreMBP was generated by mutagenesis using the Stratagene Quik Change site-directed mutagenesis protocol. MBP was purified using an osmotic shock procedure (19). preMBP was purified by amylose affinity chromatography using 10 mM maltose for elution (20). Purified protein was stored at -70°C and the bound maltose was removed by passing it over a PD10 (Amersham Biosciences) column in CGH10 buffer containing 3 M GdmCl at pH 7.2. Maltose removal was confirmed by refolding the protein and measuring the fluorescence emission spectrum (21).

Buffers and Solutions. All kinetic and equilibrium experiments were carried out in the native buffer, CGH10, pH 7.2 containing 150 mM sodium chloride. MBP unfolding was carried out for not less than 2 h in native buffer containing 2 M GdmCl at room temperature. Maltose-free preMBP in 3 M GdmCl obtained from the PD10 column was used directly as unfolded preMBP for further study. Concentration

of preMBP was determined from the absorbance value at 280 nm and an extinction coefficient of $66\,350\text{ M}^{-1}\text{cm}^{-1}$ (22). ϵ_{280} of MBP can be used for preMBP since the signal peptide does not contain Trp or Tyr residues. Concentration of GdmCl was determined by refractive index measurements. All buffers were filtered through $0.22\ \mu\text{m}$ filters, and degassed buffers were used for the stopped flow kinetic experiments.

Mass Spectroscopy and Dynamic Light Scattering (DLS). ESI-MS was performed on a Q-TOF II machine from Micromass. DLS was performed on the refolded proteins (at a minimum concentration of $10\ \mu\text{M}$) on a Dyna Pro-99 instrument at 25°C (Protein Solutions Ltd.). Samples were spun at 14 000 rpm for 10 min and filtered through a $0.02\ \mu\text{m}$ filter. Data were acquired for 3 s per data point at a sensitivity of 90%. All fluctuations in intensities greater than 15% were marked excluded and not used for the data analysis. At least 40 points were used to derive the hydrodynamic radius. Dyna LS software (Protein Solutions Ltd.) was used for the data analysis.

Analytical Gel Filtration. MBP and preMBP were subjected to gel filtration chromatography using an analytical Superdex-75 column (Amersham Pharmacia, column volume, $V_i = 24\ \text{mL}$) on a Duo Flow FPLC system (BIORAD). The column was equilibrated with CGH10 buffer, pH 7.2 containing 150 mM sodium chloride and 10 mM maltose. A total of $20\ \mu\text{g}$ of protein in a volume of $200\ \mu\text{L}$ was loaded on the column and eluted at a flow rate of $0.4\ \text{mL}/\text{min}$. The void volume (V_0) for the column was estimated to be $8.7\ \text{mL}$ using blue dextran.

Proteolytic Digestion. Eight micrograms each of refolded MBP and preMBP were subjected to controlled proteolysis in 1 mL of CGH10 buffer, pH 7.2 containing 150 mM sodium chloride at 37°C using the proteases, trypsin, chymotrypsin, proteinase K, papain, and subtilisin with an enzyme-to-substrate ratio of 2% (w/w), for the indicated time. The proteolyzed mixtures were TCA precipitated by incubating the samples with 10% TCA at -20°C for nearly two hours followed by harvesting the precipitated protein by centrifugation at $12000g$ at 4°C . The pellet was washed twice with acetone, dried, and redissolved in $30\ \mu\text{L}$ of SDS loading buffer and subjected to SDS-PAGE using a 10% gel.

CD Measurements. Far UV CD spectra were acquired on a JASCO J715A spectropolarimeter. A protein concentration of $0.5\ \mu\text{M}$ was used in a 2-mm or a 5-mm path length quartz cuvette. Measurements were done at 25°C over a wavelength range of 200–250 nm at a scan speed of $50\ \text{nm}/\text{min}$. Measurements were also done at lower scan rate of $10\ \text{nm}/\text{min}$, but the observed structural content in terms of MRE's was found to be independent of the scan rate. Data were collected with a response time of 4 s and a bandwidth of 2 nm. Each spectrum was an average of four consecutive scans. Buffer scans were acquired under similar conditions and subtracted from the protein spectrum before analysis.

For the refolding experiments, unfolded protein was refolded in 1 mL of native buffer to a final protein concentration of $0.5\ \mu\text{M}$ and GdmCl concentration of 0.15 M. The decrease in the CD signal was monitored at 222 nm. The dead time for manual mixing was about 10 s. Data were averaged over two traces.

A thermal melt was carried out with the refolded protein at a concentration of 0.6 μM in native buffer in a 1-cm path length quartz cuvette by monitoring the CD signal at 222 nm using a JASCO PTC-348WI peltier device. The sample was heated from 25 to 80 $^{\circ}\text{C}$ with a heating rate of 60 $^{\circ}\text{C}/\text{h}$. A bandwidth of 2 nm and response time of 4 s were used.

Equilibrium Unfolding Studies. A sample concentration of 0.25 μM was used for the isothermal equilibrium denaturation melts. Denaturation was carried out at various temperatures in the range of 10–42 $^{\circ}\text{C}$, by incubating the proteins at the appropriate GdmCl or urea concentration until equilibrium was established. Fluorescence was measured on a SPEX Fluoromax3 spectrofluorimeter in a 1-cm water-jacketed cell using an excitation wavelength of 280 nm and an emission wavelength of 340 nm in case of GdmCl melts and 337 nm in case of urea melts. In the urea denaturation studies, the buffer also contained 150 mM KCl. Spectral bandwidths of 1 nm for excitation and 5 nm for emission were used. Each value was the average of three consecutive measurements with a response time of 4 s.

Equilibrium unfolding as a function of GdmCl and urea concentration were also monitored at 222 nm using CD with a protein concentration of 0.4 μM in a 5-mm path length quartz cuvette. Each measurement was taken as an average of the data collected for a minute with a response time of 1 s.

Kinetic Experiments. The kinetics of refolding at 25 $^{\circ}\text{C}$ were monitored at protein concentrations of 0.2 and 0.5 μM in the manual mixing and stopped flow studies, respectively. Unfolded protein was refolded by dilution into the native buffer. The final GdmCl concentration was 0.15 M. Rapid mixing experiments were done on a Biologic SFM400 stopped flow instrument. The excitation wavelength used was 280 nm with a bandwidth of 5 nm and the emission was measured at 340 nm with a bandwidth of 10 and 20 nm for MBP and preMBP, respectively. A cuvette with a path length of 0.8 mm was used. The dead-time of the instrument was 1.4 ms.

The kinetics of unfolding of the native protein in different unfolding concentrations of GdmCl was monitored in manual mixing experiments by measuring the fluorescence at 340 nm with an excitation of 280 nm at the specified temperatures. The final protein concentration was 0.2 μM .

ANS Binding Studies. ANS binding studies were carried out on the SPEX Fluoromax3 spectrofluorimeter using excitation wavelength of either 280 or 380 nm and an emission wavelength of 475 nm. The spectral bandwidths used were 1 and 5 nm for excitation and emission, respectively. Protein and ANS concentrations used were 0.2 and 20 μM , respectively. Measured kinetic rate constants with excitation at 280 nm were identical to those obtained with excitation at 380 nm. For the delayed ANS binding study, protein refolding was initiated by dilution of the unfolded protein. After variable times of incubation (15 to 300 s), ANS was added to the refolding protein, and the ANS fluorescence was measured as described above.

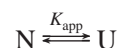
Data Analysis. Equilibrium Studies. The equilibrium data were analyzed in terms of a two-state transition using the linear extrapolation model (23) to obtain the parameters ΔG° , m , and C_m as described previously (24).

For both preMBP and MBP, m values from individual melts did not vary appreciably with temperature in the range

of 25–42 $^{\circ}\text{C}$ in case of urea melts and 15–37 $^{\circ}\text{C}$ in case of GdmCl melts, and hence all the denaturation data for each denaturant were subjected to a global fitting procedure with a single “ m ” value using the multiple function nonlinear regression of SigmaPlot for Windows scientific graphing software. The equation describing a two-state unfolding transition (25) was used to fit multiple isothermal denaturation data. The folded and the unfolded baseline parameters derived from individual fits at each of the temperatures were used to generate the fraction unfolded (f_u) as a function of denaturant concentration. The f_u data sets were subjected to the global fit regression. In the final fitting procedure, each data set was fitted to a separate two-state equation with the slopes of the baselines and free energy of unfolding as local parameters and the m value as a shared parameter across the data sets. The m value thus obtained was a temperature independent m value.

With the assumption of ΔC_p being temperature independent, the unfolding free energy (ΔG°) as a function of temperature was fit to determine the denaturation temperature (T_m) as described (25).

Thermal Melt. Unfolding as a function of temperature was monitored by observing the change in CD signal at 222 nm. The data were fit to a reversible two-state model,



where N is the native protein, U is the unfolded protein, and K_{app} is the apparent equilibrium constant. The data can be described by the equation (25):

$$Y_O = \{ (y_F + m_F T) + (y_U + m_U T) \exp \left[\frac{\Delta H^{\circ}(T_m)(T/T_m - 1) + \Delta C_p(T - T_m - T \ln(T/T_m))}{RT} \right] \} / \{ 1 + \exp \left[\frac{\Delta H^{\circ}(T_m)(T/T_m - 1) + \Delta C_p(T - T_m - T \ln(T/T_m))}{RT} \right] \}$$

where Y_O is the mean residue ellipticity measured at temperature T , y_F and y_U represent the intercepts and m_F and m_U are the slopes of the folded and unfolded baselines of the transition, respectively, T_m is the midpoint of the thermal transition, $\Delta H^{\circ}(T_m)$ is the change in enthalpy at T_m , and ΔC_p represents the change in heat capacity.

The observed data were fit to the above equation with a nonlinear least squares program using SigmaPlot for Windows scientific graphing software.

Kinetic Studies. Changes in signal intensity as a function of time in all the kinetic experiments were fit to the equation $a_{\infty} + \sum a_i \exp(-k_i t)$ or $a_0 + \sum a_i (1 - \exp(-k_i t))$, where a_{∞} represents the amplitude achieved at equilibrium, a_0 represents the amplitude change occurring in the burst phase, and a_i represents the amplitude change of the phase i occurring with an observed rate constant k_i .

RESULTS

General Features of preMBP. Because of cleavage of the signal peptide soon after preMBP synthesis, it was difficult to obtain authentic preMBP in large amounts. To overcome this problem, we have used an export-defective mutant of MBP carrying a mutation, namely, A14E, in the signal peptide. The presence of the A14E mutation in the signal peptide has been shown to decrease the rate of folding relative to that of MBP to approximately the same extent as

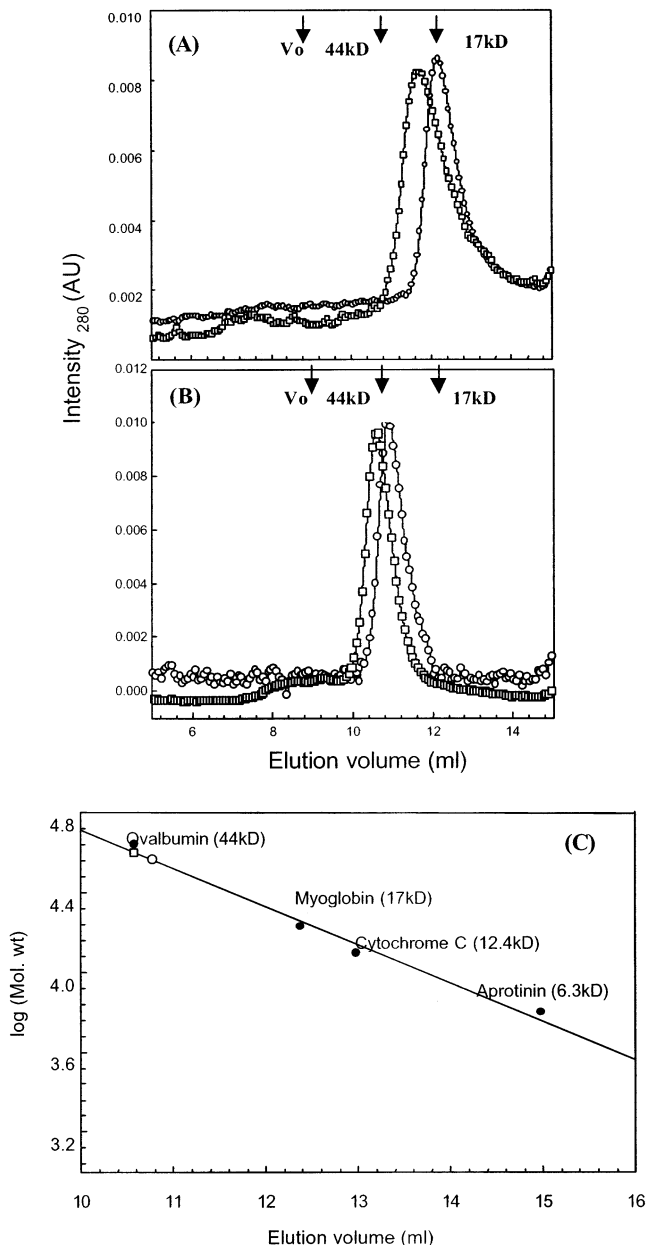


FIGURE 1: Size exclusion chromatography of MBP and preMBP. MBP (○) and preMBP (□) were analyzed on a Superdex75 gel filtration FPLC column in the absence (A) and presence (B) of 10 mM maltose, respectively. V_0 denotes the void volume for the column. (C) A standard curve for this column (in the presence of maltose) was generated by plotting the log of molecular weight against the elution volume for the following proteins (●): ovalbumin (44 kDa), myoglobin (17 kDa), cytochrome *c* (12.4 kDa) and aprotinin (6.3 kDa). The masses of MBP (○) and preMBP (□) were estimated using the elution volumes obtained in B. All chromatography was carried out using CGH10 buffer, pH 7.2, containing 150 mM NaCl with or without 10 mM maltose, at a flow rate of 0.4 mL/min.

does the wild-type signal peptide (9). SecB slows the folding of MBP but blocks the refolding of preMBP. A similar blockage effect has been reported in the case of A14EpreMBP as well (13). Hence, this mutant preMBP can be used as a substitute for authentic preMBP. The A14EpreMBP mutant protein will be referred to as preMBP hereafter. ESI-MS yielded masses of 40707 ± 1 and 43444 ± 3 for MBP and preMBP, respectively. The calculated masses were 40707.2 for MBP and 43445.6 for preMBP (inclusive of a N-terminal Met residue).

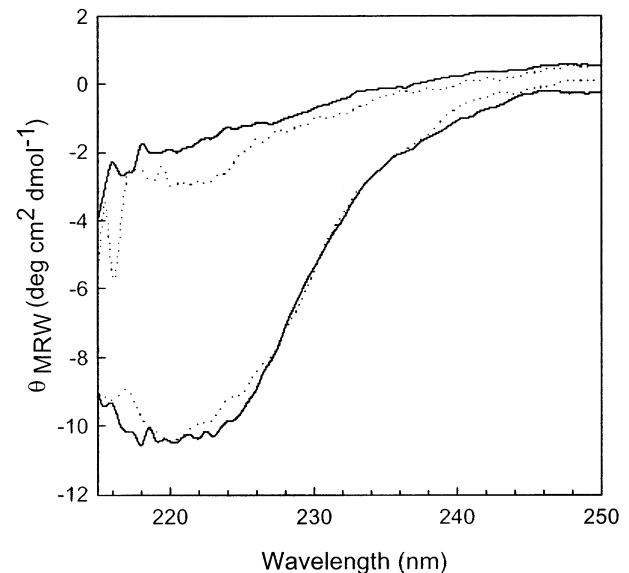


FIGURE 2: Far UV CD spectra of folded or refolded and unfolded MBP (solid line) and preMBP (dotted line) at pH 7.2, 25 °C.

preMBP was found to be aggregation prone and highly unstable. Hence, maltose bound to the protein during elution from the amylose column was removed by desalting the protein, on a PD10 column, in a GdmCl unfolded state rather than by extensive dialysis under native conditions. Maltose binding to MBP and preMBP is accompanied by fluorescence quenching and a red shift (21). Fluorescence emission spectra of the refolded protein confirmed the complete removal of maltose. Refolded preMBP was confirmed to be aggregate free by Superdex75 gel filtration chromatography (Figure 1A), absence of ANS binding (data not shown), and absence of a dependence of refolding kinetics on protein concentration (data not shown). The maximal protein concentration in the peak eluted from the gel filtration column was about $0.7 \mu\text{M}$. Because both MBP and preMBP are carbohydrate binding proteins, they tend to elute later than expected on gel filtration columns (data not shown). To reduce the interaction between the protein and column beads, gel filtration was also carried out in the presence of 10 mM maltose. In the presence of maltose, both proteins eluted at the expected volumes of 10.6 and 10.8 mL for preMBP and MBP, respectively (Figure 1B,C). Gel filtration was also carried out under denaturing conditions in the presence of 1.5 M GdmCl. Under these conditions, preMBP and MBP had similar elution volumes of 8.8 and 8.9 mL, respectively (data not shown). DLS carried out at a protein concentration of $10 \mu\text{M}$ yielded radii of 2.9 ± 0.6 and 3.2 ± 0.1 nm for the folded MBP and preMBP, respectively, confirming the monomeric nature of these proteins.

The far UV CD spectrum of refolded preMBP was found to be similar to that of MBP in the native state, indicating that the proteins have similar structure (Figure 2). Refolded preMBP was further found to be active, and Scatchard plot analysis showed that it also binds maltose at a stoichiometry of 1:1 with an affinity similar to that of MBP or the wild-type preMBP (26) (data not shown).

Refolding of MBP and preMBP was found to be reversible under the conditions used in the study. In the case of preMBP, since the refolded protein was used, reversible folding was also confirmed by repeated refolding and

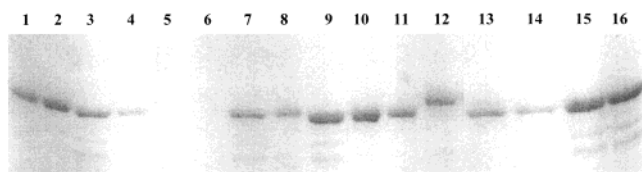


FIGURE 3: Proteolytic digestion of MBP and preMBP. 10% SDS-PAGE showing digest of MBP and preMBP performed at 37 °C. Lanes 1 and 2, papain digest of preMBP, incubation time 15 and 60 min, respectively; lanes 3 and 4, papain digest of MBP, incubation time 15 and 60 min, respectively; lane 5, papain; lane 6, chymotrypsin; lanes 7 and 8, chymotrypsin digest of preMBP, incubation time 1 and 4 h, respectively; lanes 9 and 10, chymotrypsin digest of MBP, incubation time 1 and 4 h, respectively; lane 11 undigested MBP; lane 12 undigested preMBP; lanes 13 and 14, trypsin digest of preMBP, incubation time 1 and 4 h, respectively, and lanes 15 and 16, trypsin digest of MBP incubation time 1 and 4 h, respectively. The apparent difference in the amount of total protein in the various lanes is due to losses involved during TCA precipitation.

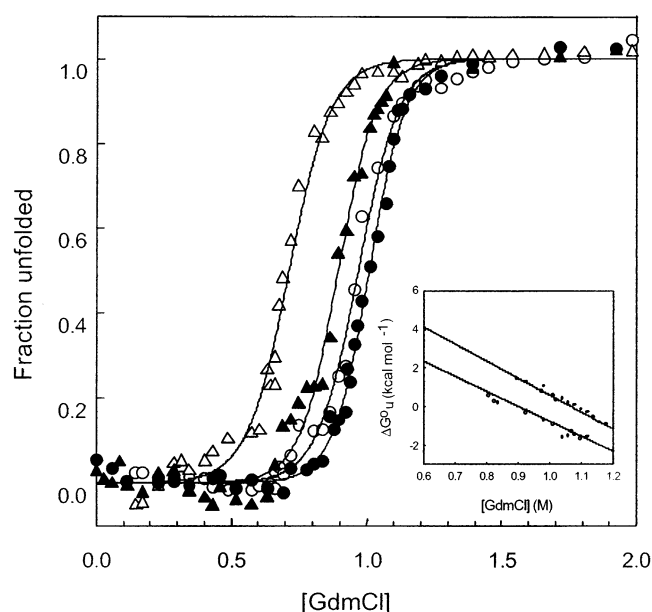


FIGURE 4: Representative GdmCl-induced denaturation curves of MBP (filled symbols) and preMBP (open symbols) at 25 °C (circle) and 37 °C (triangle) at pH 7.2. The refolding transition was monitored by a change in the fluorescence at 340 nm with excitation at 280 nm. Continuous lines indicate global fits to the data using the two-state transition analysis described in the text. Inset shows linear extrapolation of the free energy of unfolding (ΔG_u) as a function of the GdmCl concentration at 25 °C for MBP (filled circle) and preMBP (open circle).

unfolding. Unfolded protein from the PD10 column was refolded and was subjected to a second round of unfolding and refolding reaction. The rate of refolding and the relative amplitudes of the folding phase were found to be unaffected by multiple rounds of refolding and unfolding after appropriate dilution corrections (data not shown). The rate of refolding was found to be independent of the protein concentration over a 10-fold concentration range. Also the amplitude of the slow folding phase was found to be linear as a function of protein concentration.

Proteolysis was carried out using trypsin, chymotrypsin, proteinase K, papain, and subtilisin at 37 °C (Figure 3). Under these conditions, the signal peptide in preMBP is rapidly cleaved. Following cleavage of the signal peptide preMBP, which now lacks the major portion of the signal

Table 1: Comparison of Thermodynamic Parameters for the GdmCl (A) and Urea (B) Denaturation of MBP and preMBP as a Function of Temperature^{a,b}

(A) GdmCl Denaturation					
T	MBP		preMBP		
	ΔG°	ΔG°	$\Delta \Delta G^\circ$ ^c	ΔC_m ^d	
15	9.1 ± 0.3	7.3 ± 0.3	1.8	0.08	
20	9.3 ± 0.3	7.6 ± 0.04	1.6	0.05	
25	8.9 ± 0.3	7.3 ± 0.5	1.6	0.06	
30	8.5 ± 0.2	6.9 ± 0.5	1.6	0.05	
37	7.9 ± 0.2	5.5 ± 0.2	2.5	0.17	
(B) Urea Denaturation					
T	MBP		preMBP		
	ΔG°	-m (MBP)	ΔG°	$\Delta \Delta G^\circ$ ^a	ΔC_m ^b
10	9.1 ± 0.7	2.7 ± 0.2	9.2 ± 0.3	-0.1	0.9
15	9.2 ± 0.9	2.8 ± 0.3	10.1 ± 0.4	-0.9	0.6
20	10.4 ± 0.3	3.1 ± 0.3	10.9 ± 0.4	-0.5	0.4
25	16.9 ± 0.8	5.2 ± 0.2	10.0 ± 0.5	6.9	0.4
30	15.9 ± 0.8	5.2 ± 0.2	10.2 ± 0.5	5.7	0.2
37	15.0 ± 0.7	5.2 ± 0.2	8.7 ± 0.4	6.3	0.4
42	13.6 ± 0.6	5.2 ± 0.2	7.3 ± 0.4	6.2	0.5

^a Data were fit to a two-state model as described in ref 24. Error shown is the standard error from the fit. C_m values were calculated using the m values. In case of the GdmCl melts, m values of -8.9 ± 0.3 and -7.7 ± 0.3 kcal mol⁻¹ M⁻¹ for MBP and preMBP, respectively, were used. In case of the urea melts, m value of -3.6 ± 0.2 kcal mol⁻¹ M⁻¹ for preMBP and a temperature-dependent m value for the temperatures 10–20 °C and a global value of -5.2 ± 0.2 kcal mol⁻¹ M⁻¹ in the temperature range of 25–42 °C for MBP were used. ^b Units are as follows: T (°C), ΔG° (kcal/mol), $\Delta \Delta G^\circ$ (kcal/mol), ΔC_m (M). ^c $\Delta \Delta G^\circ = \Delta G^\circ(\text{MBP}) - \Delta G^\circ(\text{preMBP})$. ^d $\Delta C_m = C_m(\text{MBP}) - C_m(\text{preMBP})$.

peptide, and MBP are digested with similar kinetics. This suggests that in the folded state, the signal peptide is accessible to proteases and does not interact with the rest of the protein. Refolded preMBP was thus confirmed to be similar to the wild-type precursor with respect to all the reported features of the precursor form (9, 13, 20, 27).

Isothermal Equilibrium Denaturation Studies. GdmCl Induced Unfolding. Isothermal GdmCl induced equilibrium unfolding studies were carried out at five different temperatures. Initially, each data set at a given temperature was fit locally for the parameters as described (24). These analyses showed that within experimental error the m value did not change over the temperature range used in this study. The data sets were then refit globally for a common m value linked across all the temperatures. The lines in Figure 4 represent the results of the global fitted data. The globally determined m value was in good agreement with the average m value derived from individual fits. The C_m values were found to be identical for the individual and global fits, this further validates the global fitting of the data with a temperature-independent m value derived from individual fits. The thermodynamic parameters ΔG° and ΔC_m at each temperature are indicated in Table 1A. preMBP was found to be destabilized by nearly 2 ± 0.2 kcal/mol relative to MBP. The unfolding transition was also monitored using the CD signal at 222 nm. Plots of fraction unfolded (f_u) as a function of concentration of GdmCl using fluorescence and CD were coincident, indicating that both MBP and preMBP equilibrium denaturation is well described by a two-state unfolding mechanism (Figure 5).

A large m value indicates a highly cooperative unfolding transition for both the proteins. The m value was found to

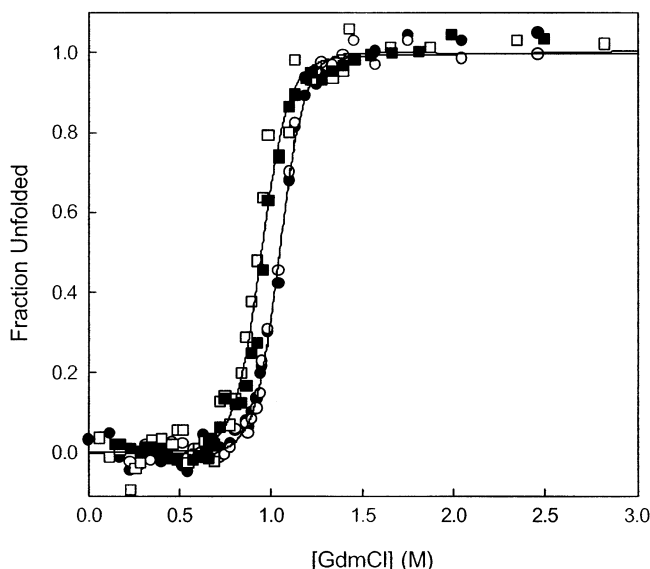


FIGURE 5: Fraction unfolded of MBP (circle) and preMBP (square) as a function of GdmCl concentration obtained from fluorescence at 340 nm (closed symbols) and CD at 222 nm (open symbols). A continuous line represents the fit to the data. Close agreement in the f_u 's obtained from both CD and fluorescence measurements validates the two-state unfolding approximation for both the proteins.

be smaller in magnitude by about $1.2 \pm 0.4 \text{ kcal mol}^{-1} \text{ M}^{-1}$ for preMBP in comparison to MBP. The m value is believed to be correlated with the surface area exposed upon unfolding (28). A lower m value for preMBP suggests that a smaller amount of surface area is exposed upon denaturation of preMBP. Because the signal peptide is solvent exposed in the native state, it suggests that the difference in the m value reflects a difference in the denatured states of the two proteins. The lower m value for preMBP may indicate that the unfolded state of preMBP is more compact and stabilized in comparison to the unfolded state of MBP.

Urea-Induced Unfolding. The difference in stability of preMBP and MBP was also monitored using isothermal urea-induced denaturation in the temperature range of 10–42 °C (Table 1B). In case of MBP, the m value was found to be temperature dependent. However the data in the temperature range of 25–42 °C could be fitted globally for a common m value as described above for the GdmCl melts (Figure 6). A good agreement in the m values and C_m from the individual and global fits validated the global fitting procedure in the higher temperature range. At temperatures below 25 °C, the m values for MBP from individual fits were appreciably lower than from the global fit value; hence, in this temperature range individual m values were used. Consequently, in the temperature range of 10–20 °C, MBP and preMBP appear to have similar ΔG° values. However, MBP consistently has a substantially higher C_m than preMBP even in this temperature range. We therefore believe that MBP is more stable than preMBP even in the temperature range of 10–20 °C, although we currently cannot explain the large decrease in m value observed in this temperature range. Comparison of stability of the two proteins in the temperature range of 25–42 °C where global fitting procedures are used indicates that preMBP was destabilized by about $6.3 \pm 0.5 \text{ kcal/mol}$ relative to MBP. Similar to the GdmCl denaturation studies, a lower m value ($\Delta m = 1.6 \pm 0.2 \text{ kcal mol}^{-1} \text{ M}^{-1}$)

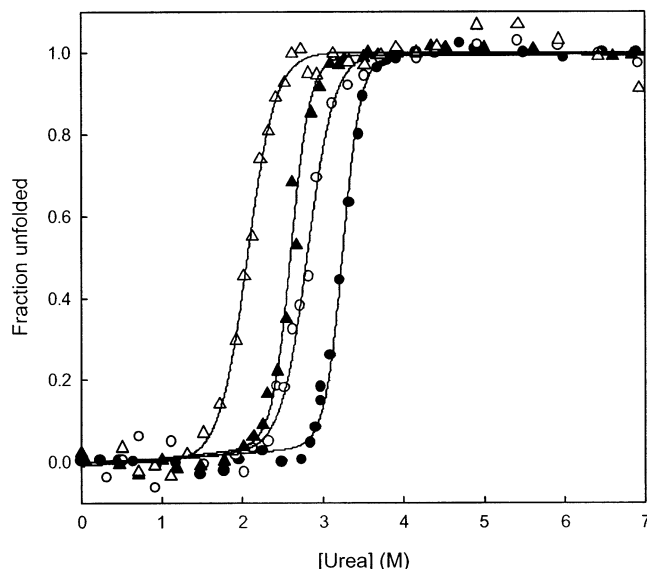


FIGURE 6: Representative urea-induced denaturation curves of MBP (filled symbols) and preMBP (open symbols) at 25 °C (circle) and 42 °C (triangle) at pH 7.2. The refolding transition was monitored by a change in the fluorescence at 337 nm with excitation at 280 nm. Continuous lines indicate global fits to the data using the two-state transition analysis described in the text.

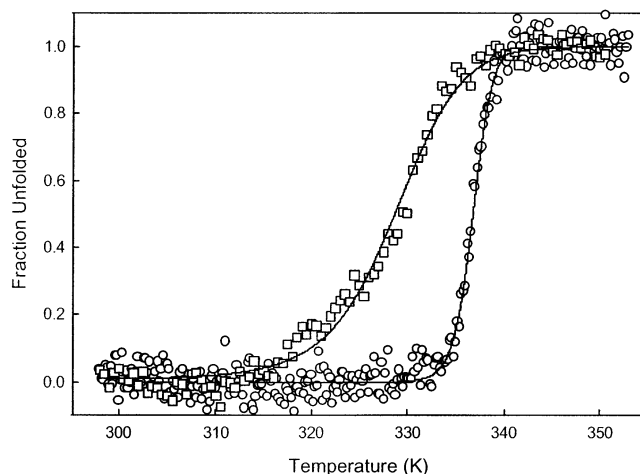


FIGURE 7: Thermal denaturation of MBP (○) and preMBP (□). Data were collected by monitoring ellipticity at 222 nm as a function of temperature. Lines represent two-state fits of the data as described in the text.

was observed for preMBP in the urea denaturation studies also, consistent with a greater compaction of the unfolded state of preMBP in comparison to that of MBP. Urea-mediated denaturation was also confirmed to be a two-state unfolding process for both MBP and preMBP since the denaturation profiles monitored by CD at 222 nm and fluorescence were identical (data not shown).

Equilibrium Thermal Denaturation. The lower stability of preMBP was also confirmed by thermal denaturation studies of both the proteins monitored by CD measurement at 222 nm (Figure 7). Thermal denaturation of MBP was reversible, but thermal denaturation of preMBP was found to be irreversible. preMBP precipitates at higher temperatures. The presence of a hydrophobic stretch of amino acids in the signal peptide leads to irreversible aggregation upon thermal unfolding, probably because of the interactions of the signal peptide with other hydrophobic regions that become exposed upon unfolding.

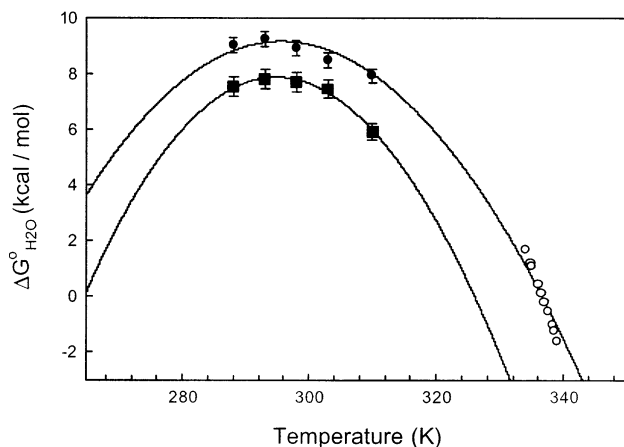


FIGURE 8: Stability curve of MBP (●) and preMBP (■) at pH 7.2. In case of MBP, closed and open symbols are the data from the isothermal GdmCl denaturation and thermal denaturation, respectively. The solid lines are fits of the data to the Gibbs-Helmholtz equation as described previously (24).

The T_m and $\Delta H^\circ(T_m)$ for MBP were found to be in good agreement with the values obtained from the calorimetric measurements. An apparent T_m was calculated from the thermal melt of preMBP by CD (Figure 7). T_m for preMBP thus calculated was found to be about 8 °C lower than that of MBP, emphasizing the destabilization of preMBP with respect to MBP. As with GdmCl and urea denaturation, thermal denaturation for preMBP was also much less cooperative than for MBP.

Conformational Stability. In the case of MBP, using the thermal denaturation data, the free energy of unfolding (ΔG°) was calculated at various temperatures in the transition zone of thermal unfolding. These are shown in Figure 8 (filled circle symbols). These free energy values were then combined with the free energy values obtained from the global fit of the isothermal GdmCl denaturation data, shown in filled circle symbols in Figure 8, to generate the stability curve. The composite data were then fit to obtain the thermodynamic parameters over a wide temperature range, 10–65 °C. There is a small but systematic deviation of ΔG° values derived from the thermal melt data from the fitted stability curve. This might be due to differences in GdmCl and thermally denatured states. Values of T_m , ΔH_m , and ΔC_p derived from the MBP stability curve shown here are 63.4 ± 1.5 °C, 143 ± 7 kcal/mol, and 3.2 ± 0.3 kcal mol⁻¹ K⁻¹. For comparison, more accurate calorimetric values are 63.1 ± 0.1 °C, 207 ± 10 kcal/mol, and 4.7 ± 0.9 kcal mol⁻¹ K⁻¹ (18). Since the thermal denaturation of preMBP was found to be irreversible, a similar procedure of combining the GdmCl denaturation data with the thermal melt data was not carried out and only the isothermal GdmCl melt data was used to generate the stability curve for preMBP. For the preMBP stability curve, values of T_m , ΔH_m , and ΔC_p were 55.7 ± 1.5 °C, 162 ± 11 kcal/mol, and 4.9 ± 0.6 kcal mol⁻¹ K⁻¹. From the MBP data, it is clear that values of T_m from the stability curve are more accurate than the ΔH_m and ΔC_p . The two T_m values, calculated from the stability curve and the thermal melt (63.4 and 63.6 °C, respectively, in case of MBP and 55.7 and 55 °C, respectively, in case of preMBP) were in close agreement.

The stability curve was also generated from the isothermal urea denaturation data following a similar procedure as

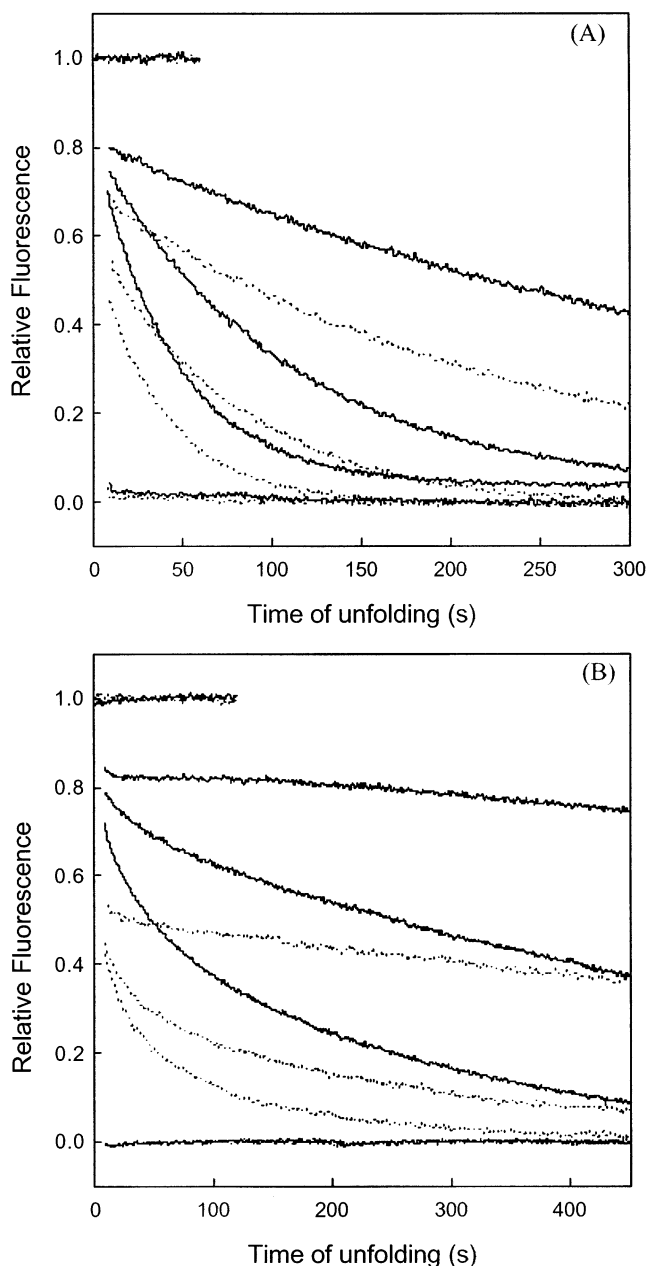


FIGURE 9: Kinetics of unfolding of MBP (solid lines) and preMBP (dotted lines) at 25 °C (A) and 10 °C (B). In both panels, from top to bottom are traces for the unfolding of the proteins to the final GdmCl concentrations of 0.01, 1.5, 1.8, 2.0, and 3.0 M, respectively. Fluorescence values were normalized between 0 and 1.0, with the native protein fluorescence taken as 1.0 and the unfolded protein steady-state fluorescence in 3.0 M GdmCl as 0.0.

described above. The T_m values thus obtained were 55.5 and 63.5 °C for preMBP and MBP, respectively (data not shown) similar to those obtained from either GdmCl melts or the thermal melts described above.

Unfolding Kinetics. MBP and preMBP have eight tryptophan residues. As the protein unfolds, these buried residues become exposed to the solvent, and the intrinsic Trp fluorescence decreases because of solvent quenching. Unfolding kinetics were monitored by following the reduction in the fluorescence signal during the unfolding of the protein from the native state to different unfolding GdmCl concentrations at 25 and 10 °C (Figure 9).

The apparent rate constant increases with an increase in the final GdmCl concentration. preMBP unfolding rate

Table 2: Kinetic Parameters of Unfolding of MBP and PreMBP at Different GdmCl Concentrations Monitored by Fluorescence Using Manual Mixing at 25 °C (A) and at 10 °C (B)

(A) 25 °C			
[GdmCl] (M) ^a	MBP k^b (s ⁻¹)	preMBP k^b (s ⁻¹)	a_0^c
2.2	0.059 ± 0.009	0.044 ± 0.009	0.41 ± 0.01
2.0	0.021 ± 0.003	0.025 ± 0.003	0.39 ± 0.12
1.8	0.011 ± 0.002	0.011 ± 0.002	0.28 ± 0.02
1.5	0.003 ± 0.001	0.002 ± 0.001	0.25 ± 0.07
(B) 10 °C			
[GdmCl] (M) ^a	MBP ($k_i \times 10^3$) ^d s ⁻¹ (a_i)	preMBP ($k_i \times 10^3$) ^d s ⁻¹ (a_i)	a_0^c
2.0	25.0 ± 1.4 (0.3)/ 3.35 ± 0.07 (0.7)	44.0 ± 8.5 (0.48)/ 9.2 ± 2.6 (0.52)	0.28 ± 0.03
1.8	32.0 ± 4.2 (0.12)/ 1.40 ± 0.0 (0.88)	33.0 ± 5.6 (0.39)/	0.27 ± 0.06
1.5 ^e	0.42 ± 0.001	0.95 ± 0.07	0.29 ± 0.001

^a Unfolding reaction was initiated by a GdmCl concentration jump from 0 M to the final GdmCl indicated. Data were fit to exponential equation as described in the text. ^b Each reading was an average of three independent experiments, and the error shown is the standard deviation of the mean value. ^c a_0 represents the amplitude of the burst phase observed in case of preMBP. The fluorescence signal was normalized to 1 for the native protein and a_0 was calculated with respect to the expected signal from the native baseline in the GdmCl equilibrium melt data. No burst phase was observed for unfolding of MBP. ^d At 10 °C, unfolding was typically biexponential. Hence, rate constants (k_i) and relative amplitudes (a_i) for both phases are indicated. ^e Unfolding of the proteins at a final GdmCl concentration of 1.5 M at 10 °C was a very slow process, and the final fitted fluorescence value at saturation in 1.5 M GdmCl indicated a residual amplitude of 23 and 8% for MBP and preMBP, respectively, relative to the corresponding unfolded state fluorescence. This shows the presence of a very slow phase, which could not be quantitated in the time scale of measurement of the unfolding experiment. Samples were incubated for an additional 20 h to confirm that the expected unfolded state fluorescence value was attained.

constants were found to be similar to those of MBP at 25 °C (Figure 9A, Table 2A). However, there was a burst phase change during the unfolding of preMBP in the dead time of the fluorescence measurement, which was not present in the case of MBP. Figure 10 shows an overlay of the kinetic amplitudes of unfolding onto the equilibrium amplitudes. For both MBP and preMBP, the fluorescence intensity at the endpoint ($t = \infty$) of the kinetic traces fall on the equilibrium unfolding baseline, indicating that the kinetic unfolding data have been measured to completion. The fluorescence intensity at the start point of the kinetic trace ($t = 0$) was obtained from back extrapolation of the fitted data to $t = 0$. In the case of MBP, the start points of the kinetic unfolding trace fall on the native baseline of the equilibrium data (Figure 10A). For preMBP, these were appreciably lower than that of the native baseline (Figure 10B).

Unfolding of preMBP was found to be faster than MBP at 10 °C (Figure 9B). Similar to the unfolding at 25 °C, burst phase changes were observed only in case of preMBP and not MBP even at 10 °C (Table 2B). Stopped flow measurements to observe unfolding could not be carried out due to the unavailability of aggregation free refolded preMBP at high concentrations. Nevertheless, the presence of a large burst phase in the manual mixing experiment indicates that a fast unfolding phase is associated with the preMBP unfolding. Hence, in contrast to the earlier report (6), signal

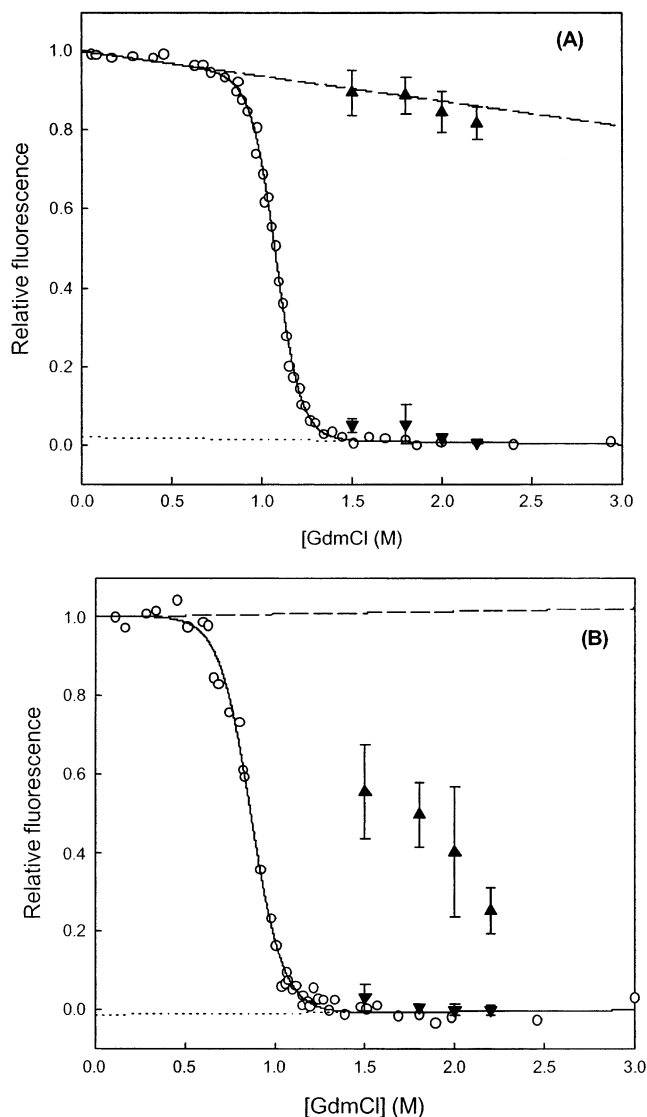


FIGURE 10: Burst phase changes in fluorescence during the unfolding of MBP (A) and preMBP (B) at pH 7.2, 25 °C. The kinetic unfolding traces were extrapolated to $t = 0$, and the extrapolated value was compared to the corresponding extrapolated value (at that GdmCl concentration) of the baselines from the equilibrium melt. In the absence of any burst phase intermediate, the two values should be identical. GdmCl-induced equilibrium unfolding (○); $t = 0$ points of kinetic unfolding traces (▲) and $t = \infty$ points of kinetic unfolding traces (▼). The continuous line through the (○) represents the fit data of the equilibrium melt. Also indicated are the baselines for the equilibrium data; dash line indicates the folded baseline and dotted line unfolded baseline. Fluorescence values were normalized between 0 and 1.0, with the native protein fluorescence taken as 1.0 and the unfolded protein fluorescence in 3.0 M GdmCl as 0.0.

peptide affects the unfolding as well as refolding kinetics of MBP.

Refolding Kinetics of MBP. Refolding of MBP and preMBP were monitored by CD, intrinsic Trp fluorescence, and binding of the hydrophobic dye, ANS. All the kinetic parameters are listed in Table 3.

Refolding data for MBP showed the presence of a large burst phase change, indicating the formation of a collapsed intermediate within a few milliseconds of denaturant dilution. This is followed by a major slow folding phase occurring with a rate constant of 0.03 s⁻¹. This rate constant was found to be independent of protein concentration and the probe used

Table 3: Kinetic Parameters of Refolding of MBP and preMBP at 298 K, pH 7.2 Monitored Using CD Measurement at 222 nm, Fluorescence at 340 nm, and ANS Fluorescence at 475 nm^a

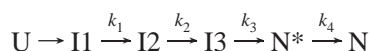
kinetic param	CD ^b		Trp fluoresc		ANS fluoresc ^b	
	MBP	preMBP	MBP	preMBP	MBP	preMBP
a_0^c	0.3	0.58	0.52	0.42	1.0	1.0
a_∞^c	1.0	1.0			0.0	0.0
a_1^d			0.03			
k_1			4.7 ± 1.3^e			
a_2			0.1			
$k_2 \times 10$			3.7 ± 0.1			
a_3	0.7		0.33		0.7	
$k_3 \times 10^2$	3 ± 0.2		3 ± 0.1		3 ± 0.3	
a_4		0.42		0.58	0.3	
$k_4 \times 10^3$		5.3 ± 0.1		7.3 ± 0.6	6 ± 0.1	5 ± 0.1

^a Data were fit to equations as described in the data analysis. Units for the rate constants are s⁻¹. ^b CD and ANS fluorescence measurements were conducted only in the manual mixing mode. ^c a_0 and a_∞ are the burst phase change and steady-state amplitude, respectively. ^d a_i ($i = 1-4$) represents the amplitude change associated with a phase i which occurs with a rate constant k_i . ^e Error shown is the standard error from the fit.

for the measurement. Since CD and fluorescence measurements yield the same rate constant, this implies that the protein acquires both secondary and tertiary structure simultaneously during the slow phase. A similar rate constant observed in the ANS binding experiment indicates that in this phase, restructuring of the collapsed chain occurs with removal of 70% of the previously bound ANS molecules. ANS binding also revealed the presence of an additional very slow phase during which the remaining 30% ANS molecules are ejected from the protein. This probably involves the slow rearrangement in the structure to attain the final native form of the protein. ANS binding to the late kinetic intermediates during the folding of protein was investigated by delayed addition of ANS to the refolding protein (data not shown). The rate constants of the two phases were found to be independent of the time of addition of ANS. The fluorescence intensity at the time of ANS addition was calculated from the fitted data and compared to the fluorescence value when ANS was present in the refolding buffer at time $t = 0$. The fluorescence intensities were found to be in close agreement. This indicates that the presence of ANS does not affect the refolding process and gives a true picture of hydrophobic collapse occurring in the slow folding phase.

To further investigate the presence of any fast phase in the folding pathway, refolding was examined by stopped flow fluorescence measurements (Figure 11A). MBP refolding was found to involve two more phases (Figure 11B).

On the basis of these observations, a minimal folding scheme can be proposed as



Here I1 is a collapsed form of the protein formed within a few milliseconds. I1 has exposed hydrophobic surface and undergoes a minor structural rearrangement to yield I2 which in turn goes to I3. I3 folds slowly with a rate constant of 0.03 s⁻¹ to give a native like state N*. N* has identical secondary and tertiary structure to the native state but contains some exposed hydrophobic surface as indicated by the ANS binding studies. N* rearranges slowly (0.006 s⁻¹)

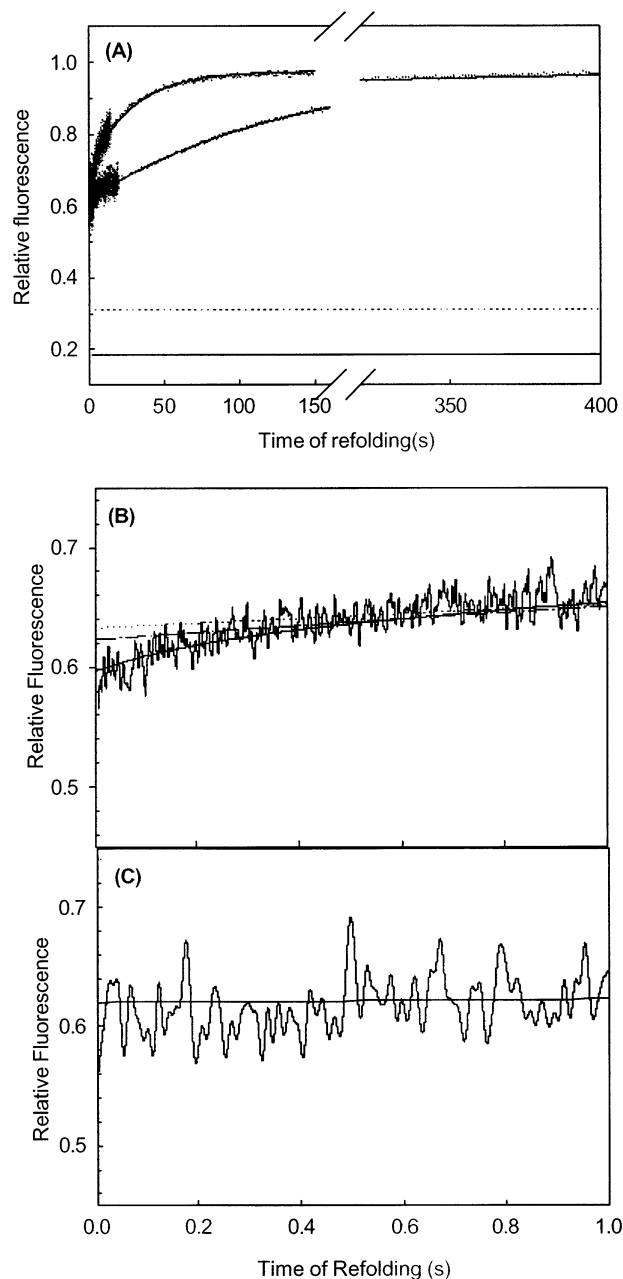
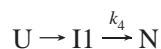


FIGURE 11: Kinetics of refolding of MBP (upper trace) and preMBP (lower trace) in 0.15 M GdmCl, pH7.2. Measurements were made on a stopped flow mixing set up as mentioned in Experimental Procedures. For each trace, the continuous line represents the fit to the data. The fluorescence signal was normalized to 1 for the native protein. (A) In case of MBP, the folding process is described by a three-exponential equation, while for preMBP a single exponential defines the entire folding process. Dotted line and continuous line represent the unfolded preMBP and MBP baseline, respectively. (B) Data observed in the first second of measurement for refolding MBP. Dotted line, dot-dashed line, and continuous line through the data represent the single-, double-, and triple-exponential fits of the data, respectively (C) Data observed in the first second of measurement for refolding preMBP. The continuous line represents the single-exponential fit of the data.

to give N. MBP is a large protein with several Pro residues. Each of the intermediates indicated above are unlikely to be single conformations, but rather are collections of different species with similar spectroscopic properties. It should also be emphasized that the above kinetic scheme is only one of many that are consistent with the spectroscopic data and others (for example, involving multiple parallel pathways

of refolding) cannot be ruled out. However, none of the conclusions of this work depend on the details of the folding kinetics.

Refolding Kinetics of preMBP. A burst phase change was also observed in the case of preMBP refolding similar to that of MBP. The collapsed state formed then folds with a rate constant of 0.007 s^{-1} to form the native protein. Stopped flow measurements show that preMBP refolding occurs in a single phase (Figure 11A,C). The intermediates I2, I3, and N* appear to be absent. The collapsed state I1 formed within a few milliseconds goes directly to the native state. CD, Trp, and ANS fluorescence monitored refolding all occur with a similar rate constant of approximately 0.006 s^{-1} (Table 3). Pulsed addition of ANS to refolding preMBP showed that the binding occurred in a single phase with a rate constant independent of the time of ANS addition. Thus, the folding of preMBP appears to follow a surprisingly simple folding pathway in contrast to the complex multiexponential folding of MBP. The folding scheme for the preMBP refolding can be represented as



Relaxation times for MBP/preMBP unfolding at 25°C were measured by manual mixing using GdmCl concentrations of 0.1–1.0 M for refolding and 1.2 and 3.0 M for the unfolding experiments. These data were in good agreement with previously measured values and are therefore not indicated.

DISCUSSION

Precursor proteins typically differ from the corresponding mature proteins by the presence of the signal peptide. In such cases, the differences in the properties of the two proteins can solely be attributed to the effect of the signal peptide on the protein. In case of RBP, the retarding effect of the signal peptide on the refolding rate of the precursor form of RBP and tryptophan substituted RBP has been demonstrated using fluorescence and CD measurements. The conformational stability of the precursor and the mature form were found to be similar in this case (7), but only data for a single melt at 25°C were presented. The only other example (to our knowledge) reporting thermodynamic characterization of a pre-protein is that of a mitochondrial pre-protein of bovine pre-adrenodoxin (adx) by DSC (8). The precursor form of adx (Padx) was found to be as active as an electron transporter as the mature adx. In this case, Padx was found to show a reduced transition temperature, denaturation enthalpy, and heat capacity in comparison to the mature adx. However, the thermal denaturation of Padx was completely irreversible, complicating the interpretation of the data. Thus, there is very limited data on the effects of signal peptides on protein stability and folding.

The folding kinetics of MBP has been previously studied using manual mixing techniques. Relaxation times for the unfolding of MBP and preMBP were shown to be very similar (9, 10), while the refolding kinetics indicated a slower folding of preMBP in comparison to MBP by a factor of 3. However, folding studies have not been carried out on the millisecond time scales. In the earlier studies of unfolding kinetics, only the relaxation rates were described, and there

was no discussion of burst phase amplitudes. Because the folding of MBP/preMBP are kinetically not two-state processes, a slower folding rate of preMBP does not necessarily imply reduced thermodynamic stability. Detailed thermodynamic characterization of authentic or mutant preMBP is also not available. The current work provides a detailed comparison between preMBP and MBP in terms of their thermodynamic stabilities, folding and unfolding kinetics. While earlier work had demonstrated only a difference in the refolding kinetics, the present study shows that there are changes in both refolding and unfolding kinetics and also in the thermodynamic stabilities of the two proteins.

Retention of maltose binding activity in preMBP suggests that the presence of signal peptide does not alter the formation of the maltose-binding pocket. This is quite reasonable, since in the crystal structure, the N-terminus is far away from the maltose-binding site and the signal peptide is at the N-terminus of the protein (29). Resistance of the refolded preMBP to various proteases used in the current study is consistent with the earlier proteolytic digestion studies of preMBP (27, 30, 31). The present data indicate that the refolded protein achieves a stable, monomeric tertiary conformation with an exposed signal peptide.

preMBP is destabilized by 20–40% in comparison to MBP, as indicated from the isothermal denaturation studies. Lowered stability is also evident by the decrease in the apparent melting temperature by 8°C . This decrease was both predicted by the stability curve and confirmed by monitoring thermal unfolding using the CD signal at 222 nm. From the equilibrium data, a reduction in the m value indicates that a smaller amount of surface area is exposed upon unfolding of preMBP relative to MBP. Analyses of signal peptides from various sources show that these have diverse sequences with certain conserved features such as the presence of a positively charged N-terminus, a large central hydrophobic stretch, and a signal peptidase recognition site. In the unfolded state, it is possible that the hydrophobic region of the signal peptide interacts with other hydrophobic regions of the protein. This kind of stabilization of the unfolded state can occur preferentially in the precursor form and can thus account for a lower stability as well as a lower m value for preMBP. Gel filtration studies under denaturing conditions did not show any appreciable differences in elution volume between MBP and preMBP. However, given the conformational diversity and dynamic nature of the denatured state, it may be difficult to detect transient interactions between signal peptide and the rest of the protein using this technique.

In addition to interactions in the unfolded state, it is also possible that the signal peptide may destabilize the native state of the protein. For example, it is possible that removal of the charged amino terminus from its location in MBP to a different location in preMBP may result in protein destabilization. Future studies with chemically synthesized signal peptides will help clarify these issues. It has been previously suggested that changes in the m value upon mutation/alteration of the protein sequence may also result from the formation of equilibrium intermediates (32–34). In the present study, there is no direct evidence for the formation of equilibrium intermediates during denaturant mediated unfolding of preMBP as denaturation followed by CD and Trp fluorescence is coincident. preMBP has fewer

detectable kinetic folding intermediates than MBP but at least one burst phase unfolding intermediate. In contrast, MBP has no kinetic unfolding intermediate. Hence, for preMBP, an appreciable fraction of the protein unfolds fast within the dead time of measurement. While we cannot rule out the possibility of the presence of small amounts of an equilibrium intermediate as being the cause of the difference in the m value between MBP and preMBP, we consider this unlikely. This is because the thermal unfolding studies yield T_m 's that are in agreement with those calculated from the stability curves, which in turn are derived from the free energy values calculated from a two-state fit. In addition, the refolding rate of the major kinetic phase is about 5-fold faster for MBP, and unlike MBP a large fraction of preMBP unfolds within the dead time of manual mixing experiments. At low temperature, in addition to the burst phase, there is an increase in the unfolding rate constants for preMBP relative to MBP. All of these data suggest that the signal peptide results in both kinetic and thermodynamic destabilization of the protein.

MBP is a periplasmic protein and is translocated via the sec pathway. A completely folded protein cannot cross the membrane using this pathway and hence needs to be in a non-native translocation competent form in the cytoplasm. preMBP is the physiological substrate of SecB. The recognition site for SecB lies within the mature domain of the protein (35, 36). However, in vitro, SecB does not bind folded MBP or folded preMBP. Overexpression of cytoplasmic MBP in vivo does not interfere with the export of other periplasmic/outer membrane proteins (37). SecB slows down but does not block refolding of MBP at room temperature while it does block the refolding of preMBP (37). The interaction of SecB with preMBP and MBP is typically described by a kinetic partitioning model (13). In such a model, folding of substrate to the native state is in kinetic competition with binding to SecB, and the difference in interaction with MBP and preMBP are exclusively ascribed to differences in folding rates of the two proteins.

However, the molecular mechanism by which the signal peptide slows down the folding of the protein has remained unclear. The present experiments suggest that the hydrophobic signal peptide interacts with hydrophobic regions of the mature protein that are exposed either in the unfolded state or in collapsed intermediate(s) along the folding/unfolding pathways. Such interactions will presumably slow the folding rate and speed the unfolding rate of the protein. This interpretation is supported by the observation that denaturant m values for both urea and GdmCl mediated unfolding are appreciably lower in magnitude for preMBP relative to MBP. The appreciable destabilization of MBP by signal peptide is functionally relevant, because it enhances the likelihood of finding the protein in an unfolded translocation-competent form and may influence the interactions of the protein with the translocation machinery. From the effect of the signal peptide on the unfolded state of preMBP, it can be speculated that signal peptides may have a role in stabilizing the unfolded state of the pre-proteins. This can have a physiological significance in the export process. More evidence is required to substantiate this role of signal peptides on protein stability.

From a different perspective, the effect of the signal peptide on the mature domain of MBP also indicates that

one cannot neglect the effect of the presence of unstructured stretches of amino acids at the termini of proteins as in the case of fusion proteins or tagged proteins. Destabilization of the native protein due to the presence of a single unprocessed methionine residue at the N-terminus has been reported in case of goat α -lactalbumin expressed in *E. coli* (38), bovine α -lactalbumin (39), and MBP (40). Thus, the presence of an amino acid extension in protein may not affect its native state in terms of structure or activity, but depending on the nature of the sequence these can still have an appreciable effect on the unfolded state and hence on the stability of the protein.

REFERENCES

1. Blobel, G., and Dobberstein, B. (1975) Transfer of proteins across membranes. I. Presence of proteolytically processed and unprocessed nascent immunoglobulin light chains on membrane-bound ribosomes of murine myeloma. *J. Cell Biol.* 67, 835–851.
2. Milstein, C., Brownlee, G. G., Harrison, T. M., and Mathews, M. B. (1972) A possible precursor of immunoglobulin light chains. *Nat. New Biol.* 239, 117–120.
3. von Heijne, G., and Blomberg, C. (1979) Trans-membrane translocation of proteins. The direct transfer model. *Eur. J. Biochem.* 97, 175–181.
4. Engelman, D. M., and Steitz, T. A. (1981) The spontaneous insertion of proteins into and across membranes: the helical hairpin hypothesis. *Cell* 23, 411–422.
5. Inouye, M., and Halegoua, S. (1980) Secretion and membrane localization of proteins in *Escherichia coli*. *CRC Crit. Rev. Biochem.* 7, 339–371.
6. Park, S., Liu, G., Topping, T. B., Cover, W. H., and Randall, L. L. (1988) Modulation of folding pathways of exported proteins by the leader sequence. *Science* 239, 1033–1035.
7. Lee, H., Chi, S. W., Kang, M., Baek, K., and Kim, H. (1996) Stability and folding of precursor and mature tryptophan-substituted ribose binding protein of *Escherichia coli*. *Arch. Biochem. Biophys.* 328, 78–84.
8. Goder, V., Beckert, V., Pfeil, W., and Bernhardt, R. (1998) Impact of the presequence of a mitochondrion-targeted precursor, preadrenodoxin, on folding, catalytic activity, and stability of the protein in vitro. *Arch. Biochem. Biophys.* 359, 31–41.
9. Liu, G. P., Topping, T. B., Cover, W. H., and Randall, L. L. (1988) Retardation of folding as a possible means of suppression of a mutation in the leader sequence of an exported protein. *J. Biol. Chem.* 263, 14790–14793.
10. Diamond, D. L., Strobel, S., Chun, S. Y., and Randall, L. L. (1995) Interaction of SecB with intermediates along the folding pathway of maltose-binding protein. *Protein Sci.* 4, 1118–1123.
11. Raffy, S., Sassoon, N., Hofnung, M., and Betton, J. M. (1998) Tertiary structure-dependence of misfolding substitutions in loops of the maltose-binding protein. *Protein Sci.* 7, 2136–2142.
12. Chun, S. Y., Strobel, S., Bassford, P., Jr., and Randall, L. L. (1993) Folding of maltose-binding protein. Evidence for the identity of the rate-determining step in vivo and in vitro. *J. Biol. Chem.* 268, 20855–20862.
13. Hardy, S. J., and Randall, L. L. (1991) A kinetic partitioning model of selective binding of nonnative proteins by the bacterial chaperone SecB. *Science* 251, 439–443.
14. Collier, D. N. (1993) SecB: a molecular chaperone of *Escherichia coli* protein secretion pathway. *Adv. Protein Chem.* 44, 151–193.
15. Lecker, S. H., Driessen, A. J., and Wickner, W. (1990) ProOmpA contains secondary and tertiary structure prior to translocation and is shielded from aggregation by association with SecB protein. *EMBO J.* 9, 2309–2314.
16. Fekkes, P., den Blaauwen, T., and Driessen, A. J. (1995) Diffusion-limited interaction between unfolded polypeptides and the *Escherichia coli* chaperone SecB. *Biochemistry* 34, 10078–10085.
17. Panse, V. G., Udgaonkar, J. B., and Varadarajan, R. (1998) SecB binds only to a late nativelike intermediate in the folding pathway of barstar and not to the unfolded state. *Biochemistry* 37, 14477–14483.
18. Prajapati, R. S., Lingaraju, G. M., Bacchawat, K., Surolia, A., and Varadarajan, R. (2003) Thermodynamic effects of replace-

- ments of Pro residues in helix interiors of Maltose Binding Protein. *Proteins* 53, 863–871.
19. Kellermann, O. K., and Ferenci, T. (1982) Maltose-binding protein from *Escherichia coli*. *Methods Enzymol.* 90, 459–463.
 20. Ferenci, T., and Klotz, U. (1978) Affinity chromatographic isolation of the periplasmic maltose binding protein of *Escherichia coli*. *FEBS Lett* 94, 213–217.
 21. Szmelcman, S., Schwartz, M., Silhavy, T. J., and Boos, W. (1976) Maltose transport in *Escherichia coli* K12. A comparison of transport kinetics in wild-type and lambda-resistant mutants as measured by fluorescence quenching. *Eur. J. Biochem.* 65, 13–9.
 22. Ganesh, C., Shah, A. N., Swaminathan, C. P., Surolia, A., and Varadarajan, R. (1997) Thermodynamic characterization of the reversible, two-state unfolding of maltose binding protein, a large two-domain protein. *Biochemistry* 36, 5020–5028.
 23. Pace, C. N. (1986) Determination and analysis of urea and guanidine hydrochloride denaturation curves. *Methods Enzymol* 131, 266–280.
 24. Sheshadri, S., Lingaraju, G. M., and Varadarajan, R. (1999) Denaturant mediated unfolding of both native and molten globule states of maltose binding protein are accompanied by large ΔC_p 's. *Protein Sci.* 8, 1689–1695.
 25. Agashe, V. R., and Udgaonkar, J. B. (1995) Thermodynamics of denaturation of barstar: evidence for cold denaturation and evaluation of the interaction with guanidine hydrochloride. *Biochemistry* 34, 3286–3299.
 26. Ferenci, T., and Randall, L. L. (1979) Precursor maltose-binding protein is active in binding substrate. *J. Biol. Chem.* 254, 9979–9981.
 27. Randall, L. L., and Hardy, S. J. (1986) Correlation of competence for export with lack of tertiary structure of the mature species: a study in vivo of maltose-binding protein in *E. coli*. *Cell* 46, 921–928.
 28. Myers, J. K., Pace, C. N., and Scholtz, J. M. (1995) Denaturant m values and heat capacity changes: relation to changes in accessible surface areas of protein unfolding. *Protein Sci.* 4, 2138–2148.
 29. Spurlino, J. C., Lu, G. Y., and Quijcho, F. A. (1991) The 2.3-Å resolution structure of the maltose- or maltodextrin-binding protein, a primary receptor of bacterial active transport and chemotaxis. *J. Biol. Chem.* 266, 5202–5219.
 30. Dierstein, R., and Wickner, W. (1985) The leader region of pre-maltose binding protein binds amphiphiles. A model for self-assembly in protein export. *J. Biol. Chem.* 260, 15919–15924.
 31. Collier, D. N., Bankaitis, V. A., Weiss, J. B., and Bassford, P. J. J. (1988) The antifolding activity of SecB promotes the export of the *E. coli* maltose-binding protein. *Cell* 53, 273–283.
 32. Creighton, T. E., and Shortle, D. (1994) Electrophoretic characterization of the denatured states of staphylococcal nuclease. *J. Mol. Biol.* 242, 670–682.
 33. Soulages, J. L. (1998) Chemical denaturation: potential impact of undetected intermediates in the free energy of unfolding and m -values obtained from a two-state assumption. *Biophys. J.* 75, 484–492.
 34. Spudich, G., and Marqusee, S. (2000) A change in the apparent m value reveals a populated intermediate under equilibrium conditions in *Escherichia coli* ribonuclease HI. *Biochemistry* 39, 11677–11683.
 35. Topping, T. B., and Randall, L. L. (1994) Determination of the binding frame within a physiological ligand for the chaperone SecB. *Protein Sci.* 3, 730–736.
 36. Knoblauch, N. T., Rudiger, S., Schonfeld, H. J., Driessen, A. J., Schneider-Mergener, J., and Bukau, B. (1999) Substrate specificity of the SecB chaperone. *J. Biol. Chem.* 274, 34219–34225.
 37. Liu, G., Topping, T. B., and Randall, L. L. (1989) Physiological role during export for the retardation of folding by the leader peptide of maltose-binding protein. *Proc. Natl. Acad. Sci. U.S.A.* 86, 9213–9217.
 38. Chaudhuri, T. K., Horii, K., Yoda, T., Arai, M., Nagata, S., Terada, T. P., Uchiyama, H., Ikura, T., Tsumoto, K., Kataoka, H., Matsushima, M., Kuwajima, K., and Kumagai, I. (1999) Effect of the extra n-terminal methionine residue on the stability and folding of recombinant alpha-lactalbumin expressed in *Escherichia coli*. *J. Mol. Biol.* 285, 1179–1194.
 39. Ishikawa, N., Chiba, T., Chen, L. T., Shimizu, A., Ikeguchi, M., and Sugai, S. (1998) Remarkable destabilization of recombinant alpha-lactalbumin by an extraneous N-terminal methionyl residue. *Protein Eng.* 11, 333–335.
 40. Ganesh, C., Banerjee, A., Shah, A., and Varadarajan, R. (1999) Disordered N-terminal residues affect the folding thermodynamics and kinetics of maltose binding protein. *FEBS Lett.* 454, 307–311.

BI0360509